Evolutionary Game Theoretic Insights on the SIRS Model of the COVID-19 Pandemic

Madeo D. * **Mocenni C.** *

* *Department of Information Engineering and Mathematics*
University of Siena
Via Roma, 56, 53100 Siena Italy
(e-mail: {dario.madeo,chiara.mocenni}@unisi.it).

Abstract: The effectiveness of control measures against the diffusion of the COVID-19 pandemic is grounded on the assumption that people are prepared and disposed to cooperate. From a strategic decision point of view, cooperation is the unreachable strategy of the prisoner's dilemma game, where the temptation to exploit the others and the fear to be betrayed by them drives the people behavior, which eventually results fully defective. In this work, we integrate the SIRS epidemic model with the replicator equation of evolutionary games in order to study the interplay between the infection spreading and the propensity of people to become cooperative under the pressure of the epidemic. We find that the developed model possesses several steady states, including fully or partially cooperative ones and that the presence of such states allows to take the disease under control. Moreover, assuming a seasonal variation of the infection rate, the system presents rich dynamics, including chaotic behavior and epidemic extinction.

Keywords: Game Theory, Replicator Equation, Epidemic Models, SIRS, Bifurcations, Chaotic behavior, COVID-19.

1. INTRODUCTION

The recent world coronavirus pandemic enforced the application of control measures for restraining the virus diffusion. Although the most effective measure is recognized to be vaccinating people, additional behavioral measures have been shown to be successful for weakening and reducing the infection, such as social distancing, movement reduction, mask wearing, and so on (Funk (2010)). The application of control measures requires the organization of suitable information campaigns aimed at inducing people to adopt correct behaviors against the pandemic. To make these campaigns effective, people must behave cooperatively with respect to the limitations imposed by the governments. Unfortunately, more often, when taking decisions under strong pressure, such as in the initial phases of the pandemic, the requested efforts may activate in the population selfish mechanisms, such as the temptation to exploit the others and the fear to be betrayed. An example of these mechanisms is represented by the panic buying arisen at the beginning of the COVID-19 pandemic (see, for example, Stiff (2020)). Preventing these mechanisms requires fostering altruistic and cooperative feelings.

Nowadays, cooperation is recognized to be a crucial factor for successfully promoting the achievement of sustainable development in self-interested societies (Pennisi (2009); Hofman (2011)). The Evolutionary Game Theory (EGT) represents a natural mathematical framework to deal with this problem. Indeed, EGT provides a rigorous methodology for studying strategic interactions among people evolving over time (Hofbauer (2003); Nowak (2004)). The influence of networks on the dynamics of evolutionary games has been also investigated recently (Madeo (2019)).

The emergence of cooperation has been analyzed deeply in the framework of EGT, where the evident drawbacks of selfish behavior are highlighted in the defective prisoner's dilemma game (Killingback (2001); Boyd (2010)). The influence of structured populations has also been investigated (Otsuki (2006); Madeo (2020)) by taking into account the people interactions in a social dilemma context.

After the emergence of COVID-19 epidemic, the integration of the standard (Hethcote (2000)) or adapted (Gatto (2020); Calafiore (2020)) SIR and SIRS models of epidemics with suitable control measures for contrasting the pandemic, has started to be studied from different points of view. For example, in Della Rossa (2020) optimal control measures are identified by assuming networked populations, while in McAdams (2020) an analysis of strategic behavior during the COVID-19 pandemic has been developed from the economic perspective. Additionally, in Ye (2021) the strong interplay between the spreading dynamics of an epidemic and the collective behavioral pattern of the population has been accounted with suitable stochastic models.

In this paper, we propose a model which integrates a standard SIRS epidemic model with the replicator equation (SIRS-RE) describing the evolution over time of the cooperation in large populations. The two models are joined in two ways. The infection rate is assumed to depend on the propensity to cooperate by respecting the control measures taken by the governments, represented by the state variable of the replicator equation (RE). Moreover,

the parameters of the game payoff matrix depend on the strength of the epidemic at any time, thus the higher is the gravity of the epidemic, the higher is the propensity to cooperate.

The main findings of the study concern the evidence that cooperation is effective in contrasting the epidemic spreading. Indeed, cooperative behavior reduces the asymptotic level of infection. Moreover, the strength of the disease activates, as expected, the propensity of people to be more cooperative despite the limitations and sacrifices imposed by the government directives. Indeed, the switch from the prisoner's dilemma game to the fully cooperative harmony game is observed.

From the dynamical point of view, in the integrated model the infection peaks are reduced and delayed with respect to the natural ones, thus inducing transitory oscillating behaviors. By further assuming seasonal changes of the infection rate, as it is reasonably expected (Augeraud (2014)), a sequence of period doubling bifurcations is observed, eventually giving rise to chaotic behavior. However, as long as the strength of the seasonality is increased, a drastic reduction of the pandemic is observed, leading to its extinction.

2. THE MODEL

We consider a population of N individuals, composed of the standard three classes of the SIRS dynamics. Specifically, S, I and R are the number of susceptible, infected and recovered individuals, respectively. The equations of the model are the following (Hethcote (2000)):

$$\begin{cases} \dot{S} & = -\beta S \dfrac{I}{N} + \alpha R \\ \dot{I} & = +\beta S \dfrac{I}{N} - \gamma I \\ \dot{R} & = -\alpha R + \gamma I \end{cases}, \qquad (1)$$

where $\beta > 0$ is the infection rate, $\gamma > 0$ is the recovery rate and $\alpha > 0$ is the proportion of people who lose immunity.

We also assume that people can cooperate or defect. In particular, their behavior will change according to the observed pandemic status. We denote by $x \in [0,1]$ the share of population cooperating by respecting the restrictions imposed by government for contrasting the spread of the disease, and by $y = 1 - x$ the share of defective individuals. The behavior of people with respect to the diseases can be assumed to be ruled by the following payoff matrix, describing the outcome of the interaction between two players randomly chosen within the population:

$$B = \begin{bmatrix} 1 & \mathcal{S} \\ \mathcal{T} & 0 \end{bmatrix}, \qquad (2)$$

where $\mathcal{T}$ represents the temptation to defect and $\mathcal{S}$ is the "sucker's payoff", embodying the fear to be betrayed by others. More specifically, rows of B correspond to the strategy of player 1 (to cooperate is the first row, to defect is the second), while columns correspond to the choice of player 2. Players 1 earns 1 if both players cooperate, $\mathcal{T}$ if he defects and the opponent cooperates, $\mathcal{S}$ if he cooperates and the opponent defects, or 0 if both players defect. It is worthwhile to remark that, for $\mathcal{T} > 1$ and $\mathcal{S} < 0$, the payoff matrix (2) represents a prisoner's dilemma game, where defection is dominant, while for $\mathcal{T} < 1$ and $\mathcal{S} > 0$, the game switches to a harmony game, where cooperation is dominant. The corresponding RE (Hofbauer (2003); Nowak (2004)) reads as follows:

$$\begin{cases} \dot{x} & = x(\pi_1 - \phi) \\ \dot{y} & = y(\pi_2 - \phi) \end{cases}, \qquad (3)$$

where

$$\begin{bmatrix} \pi_1 \\ \pi_2 \end{bmatrix} = B \cdot \begin{bmatrix} x \\ y \end{bmatrix} = \begin{bmatrix} x + \mathcal{S}y \\ \mathcal{T}x \end{bmatrix}$$

represent the average payoffs π_1 and π_2 collected by the share of cooperative and defective individuals, respectively, while

$$\phi = x\pi_1 + y\pi_2 = x^2 + (\mathcal{T} + \mathcal{S})xy,$$

is the average payoff of the whole population.

Coherently with the payoff matrix (2), the evolution of the cooperation over time represented by the RE (3) can show full defection ($x = 0$ and $y = 1$) for the prisoner's dilemma case or full cooperation ($x = 1$ and $y = 0$) for the harmony game.

If we assume that the RE (3) describes the cooperation dynamics within a population experiencing a pandemic, then it is natural to assume that the ruling parameters $\mathcal{T}$ and $\mathcal{S}$ vary with respect to the perception of people regarding the strength of the infection measured by the state variable I of the SIRS model. In this regard, we can assume that the payoff matrix (2) depends on I, i.e. $B = B(I)$, and that it switches from a prisoner's dilemma game to a harmony one when the value of I exceeds a given threshold θ, according to the following definitions of the temptation and of the sucker's payoffs:

$$\mathcal{T}(I) = 1 - \mathcal{T}^0(I - \theta), \mathcal{S}(I) = -\mathcal{S}^0(I - \theta),$$

where $\mathcal{T}^0 > 0$, $\mathcal{S}^0 < 0$ and $0 < \theta < N$. In general, for $I < \theta$, B represents a prisoner's dilemma game, since $\mathcal{T}(I) = 1 - \mathcal{T}^0(I - \theta) > 1$ and $\mathcal{S}(I) = -\mathcal{S}^0(I - \theta) < 0$. That is, when the epidemics is quite low, the defection represents the "natural" choice of individuals, since the low perceived relevance of the disease does not justify the adoption of any containment measure. This fact is coherent with the fact that many people don't follow the rules, or some governments have been more laxer than others in imposing restrictions. In this sense, the threshold θ represents an important tuning parameter for the policy-maker, as it can be reduced by means of effective informative campaign on the real risk of the current sanitary crisis, thus making $I > \theta$. In this case, $B(I)$ turns to a harmony game since $\mathcal{T}(I) = 1 - \mathcal{T}^0(I - \theta) < 1$ and $\mathcal{S}(I) = -\mathcal{S}^0(I - \theta) > 0$.

As already said, cooperation corresponds to the adoption of good practices, aimed at the reduction of the disease spread, e.g. limitation of social interactions. Since in the general epidemic SIR/SIRS model, the parameter β represents the infection rate, it can be assumed to vary according to the behavior of people. More specifically, cooperation produces a reduction of the infection rate, while defection leads to an increase of it. Hence, the infection rate β depends on the cooperation x as follows:

$$\beta(x) = \beta_0(1 - mx),$$

where β_0 represents the natural infection rate of the disease, while $m \in (0,1)$ weights the influence of the
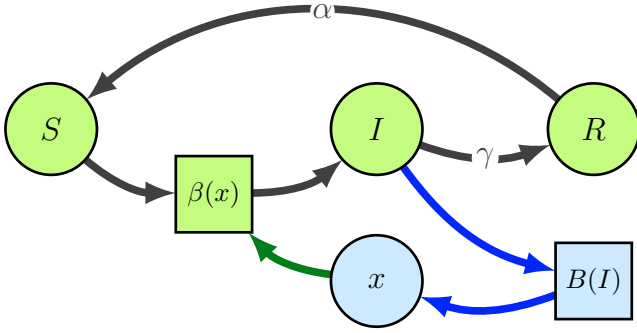
Fig. 1. Schematic representation of the proposed model. Two feedback mechanisms are at work coupling the SIRS and the RE: 1) the number of infected I influences the cooperation dynamics by changing the payoff matrix $B(I)$ (blue arrows); 2) the cooperation x influences the infection rate $\beta(x)$ (dark green arrow).

cooperation on the infection rate. Notice that $m \in (0, 1)$ guarantees that $\beta(x) > 0 \ \forall x \in [0, 1]$. In this case, the basic reproduction number is defined as follows:

$$R_0^G(x) = \frac{\beta(x)}{\gamma} = \frac{\beta_0(1 - mx)}{\gamma} = R_0(1 - mx),$$

where the superscript G denotes the presence of the game, and $R_0 = \frac{\beta_0}{\gamma}$ represents the natural basic reproduction number of the disease. The maximum of $R_0^G(x)$ is reached for no cooperation ($x = 0$), thus reducing to R_0, while the minimum of $R_0^G(x)$ is attained in presence of maximum cooperation ($x = 1$), when countermeasures against the disease are effective at the highest level.

In order to couple systems (1) and (3), we start by noticing that S can be omitted in system (1) since $S + I + R = N$, and y can be omitted in system (3), since $x + y = 1$. Then, the coupled model, hereafter called SIRS-RE, is the following:

$$\begin{cases} \dot{I} &= (\beta(x)(N - I - R) - \gamma N)\dfrac{I}{N} \\ \dot{R} &= -\alpha R + \gamma I \\ \dot{x} &= x(1 - x)((\mathcal{T}^0 + \mathcal{S}^0)x - \mathcal{S}^0)(I - \theta) \end{cases} \quad (4)$$

According to the properties of SIRS and of RE, the set $\mathcal{F} = \{[I, R, x] \in \mathbb{R}_+^3 : I + R \leq N, x \leq 1\}$ is an invariant set of system (4). Fig. 1 reports a pictorial representation of the SIRS-RE model (4).

3. ANALYSIS OF THE SIRS-RE MODEL

For the analysis of the SIRS-RE model, we assume that the natural basic reproduction number R_0 is bigger than 1, thus investigating the case for which the disease is spreading in the population without any active control measure. The system (4) has 7 steady states:

- $E_1 = [0, 0, 0]$. This is always feasible.
- $E_2 = [0, 0, 1]$. This is always feasible.
- $E_3 = \left[0, 0, \frac{\mathcal{S}^0}{\mathcal{T}^0 + \mathcal{S}^0}\right]$. This is unfeasible since $\mathcal{S}^0 < 0$ and $\mathcal{T}^0 > 0$ implies that $\frac{\mathcal{S}^0}{\mathcal{T}^0 + \mathcal{S}^0} \notin [0, 1]$.
- $E_4 = \left[\overline{\theta}, \overline{\theta}\frac{\gamma}{\alpha}, 0\right]$, where $\overline{\theta} = N\frac{\alpha}{\alpha+\gamma}\left(1 - \frac{1}{R_0}\right)$. This is feasible when $R_0 > 1$.

- $E_5 = \left[N\frac{\alpha}{\alpha+\gamma}D, N\frac{\gamma}{\alpha+\gamma}D, \frac{\mathcal{S}^0}{\mathcal{T}^0+\mathcal{S}^0}\right]$, where $D = \left(1 - \frac{\mathcal{T}^0+\mathcal{S}^0}{R_0(\mathcal{S}^0(1-m)+\mathcal{T}^0)}\right)$. This is unfeasible since $\mathcal{S}^0 < 0$ and $\mathcal{T}^0 > 0$ implies that $\frac{\mathcal{S}^0}{\mathcal{T}^0+\mathcal{S}^0} \notin [0, 1]$.
- $E_6 = \left[\underline{\theta}, \underline{\theta}\frac{\gamma}{\alpha}, 1\right]$, where $\underline{\theta} = N\frac{\alpha}{\alpha+\gamma}\left(1 - \frac{1}{R_0(1-m)}\right)$. This is feasible when $R_0(1 - m) > 1$, or equivalently when $m < \overline{m} = 1 - \frac{1}{R_0}$.
- $E_7 = \left[\theta, \theta\frac{\gamma}{\alpha}, \frac{N\alpha + R_0((\gamma+\alpha)\theta - N\alpha)}{mR_0((\gamma+\alpha)\theta - N\alpha)}\right]$. This is feasible when $\underline{\theta} \leq \theta \leq \overline{\theta}$. Notice that the previous is a well-posed interval, since $m > 0$ and $R_0 > 1$ imply that the lower bound is less than the upper one, and the upper one is positive.

Both steady states E_1 and E_2 represent the disappearing of the pandemic. Moreover, steady state E_7 is the only one having the x component in the set $(0, 1)$, thus showing an intermediate level of cooperation.

Collision of steady states

- E_1 and E_4 coincide for $R_0 = 1$.
- E_2 and E_6 coincide for $R_0(1 - m) = 1$, or equivalently, for $m = \overline{m}$.
- E_4 and E_7 coincide for $\theta = \overline{\theta}$.
- E_6 and E_7 coincide for $\theta = \underline{\theta}$.

Stability of steady states

E_1 and E_2 are unstable for any combination of the parameters since $R_0 > 1$. For E_4 and E_6, the following Theorems on their stability hold.

Theorem 1. If $R_0 > 1$ and $\theta > \overline{\theta}$, then E_4 is asymptotically stable.

Proof. The first eigenvalue of the Jacobian matrix of system (4) evaluated in E_4 is:

$$\lambda_1 = \frac{\mathcal{S}_0\left(\theta R_0(\alpha + \gamma) - N\alpha(R_0 - 1)\right)}{R_0(\alpha + \gamma)}.$$

Since $\theta > \overline{\theta}$, $\mathcal{S}_0 < 0$ and $R_0(\alpha + \gamma) > 0$, then:

$$\begin{aligned} \theta &> N\frac{\alpha}{\alpha+\gamma}\left(1 - \frac{1}{R_0}\right) &\Rightarrow \\ \theta R_0(\alpha + \gamma) &- N\alpha(R_0 - 1) > 0 &\Rightarrow \\ \frac{\mathcal{S}_0\left(\theta R_0(\alpha + \gamma) - N\alpha(R_0 - 1)\right)}{R_0(\alpha + \gamma)} &< 0 \Rightarrow \\ \lambda_1 &< 0. \end{aligned}$$

In addition, $\lambda_{2,3} = (-\delta \pm \sqrt{\delta^2 - \eta})\mu^{-1}$, where:

$$\delta = \alpha(R_0\gamma + \alpha), \quad (5)$$
$$\eta = 4\alpha\gamma(R_0 - 1)(\alpha + \gamma)^2, \quad (6)$$

and $\mu = 2(\alpha + \gamma)$. δ and μ are always positive, and η is positive since $R_0 > 1$. Hence there are two cases:

- if $\delta^2 - \eta \geq 0$, then $\sqrt{\delta^2 - \eta} < \delta$. Hence $\lambda_{2,3}$ are both real and less than 0.
- if $\delta^2 - \eta < 0$, then the real part of λ_2 and λ_3 is $-\frac{\delta}{\mu} < 0$.

Summarizing, all eigenvalues of the Jacobian matrix evaluated in E_4 have negative real part, thus E_4 is asymptotically stable. $\square$

Theorem 2. If $R_0(1 - m) > 1$ and $\theta < \underline{\theta}$, then E_6 is asymptotically stable.

Proof. The first eigenvalue of the Jacobian matrix of system (4) evaluated in E_6 is:

$$\lambda_1 = \frac{\mathcal{T}_0 \left(\theta R_0(1-m)(\alpha+\gamma) - N\alpha(R_0(1-m)-1)\right)}{R_0(1-m)(\alpha+\gamma)}.$$

Since $\theta < \underline{\theta}$, $\mathcal{T}_0 > 0$ and $R_0(1-m)(\alpha+\gamma) > 0$, then:

$$\theta < N\frac{\alpha}{\alpha+\gamma}\left(1 - \frac{1}{R_0(1-m)}\right) \qquad \Rightarrow$$
$$\theta R_0(1-m)(\alpha+\gamma) - N\alpha(R_0(1-m)-1) < 0 \qquad \Rightarrow$$
$$\frac{\mathcal{T}_0\left(\theta R_0(1-m)(\alpha+\gamma) - N\alpha(R_0(1-m)-1)\right)}{R_0(1-m)(\alpha+\gamma)} < 0 \Rightarrow$$
$$\lambda_1 < 0.$$

The values of λ_2 and λ_3 are the same as in Theorem 2, provided that in the terms δ and η (equations (5) and (6)) one must replace R_0 with $R_0(1-m)$. Recalling that by hypothesis $R_0(1-m) > 1$, then E_6 is asymptotically stable. $\square$
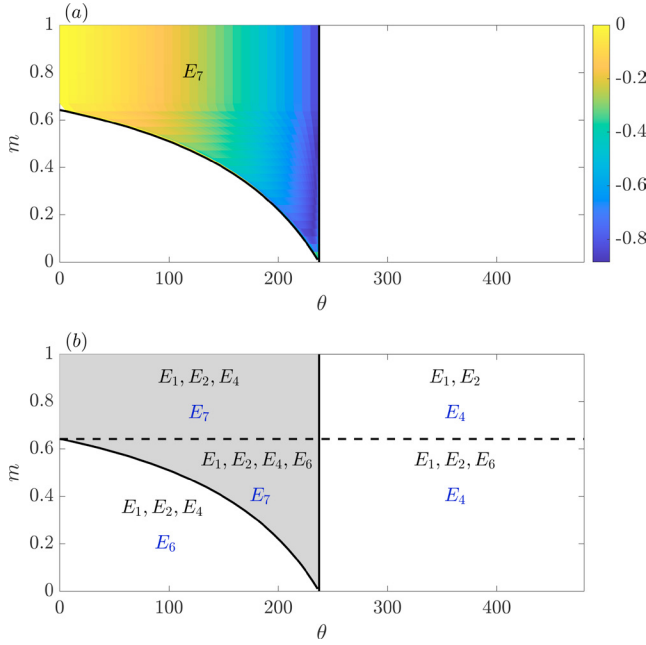

Fig. 2. (a) Maximum value of the real part of the eigenvalues of the Jacobian matrix evaluated at the steady state E_7 as a function of parameters θ and m. The value of other parameters is reported in the main text. (b) Feasibility and stability regions for each steady state. Steady states reported in black are only feasible, while stability is denoted by blue font color. The full black lines are $\theta = \underline{\theta}$ and $\theta = \overline{\theta}$, while the dashed line is $m = \overline{m}$.

In the following, we complete the stability analysis of steady states by analyzing E_7 in its feasible region with respect to the parameters m and θ. In this region, E_1, E_2 and E_4 are feasible, while E_6 is feasible only for $m < \overline{m}$. We recall that E_1 and E_2 are unstable. Moreover, thanks to Theorems 1 and 2, E_4 and E_6 (when feasible) are also unstable. Due to the boundedness of the solution ($\mathcal{F}$ is bounded and is an invariant set of system (4)), then the only candidate to be a stable steady state is E_7. Nevertheless, steady state solutions can converge also to attractive limit cycles. In subplot (a) of Fig. 2, we report the maximum real part among all eigenvalues of the Jacobian matrix evaluated at the steady state E_7 as a function

of parameters θ and m. Other parameters have been set as follows: $N = 10^4$, $\beta_0 = \frac{365}{5}$ year^{-1} = 73 year^{-1}, $\gamma = \frac{365}{14}$ year^{-1} = 26.1 year^{-1}, $\alpha = \frac{365}{365}$ year^{-1} = 1 year^{-1}, $\mathcal{T}^0 = 1.5$ and $\mathcal{S}^0 = -2$. β_0 and γ have been set according to the values reported in (Della Rossa (2020)). With this setup, the natural basic reproduction number is $R_0 = 2.8$. The reported value are always negative, thus ensuring the asymptotic stability of E_7 in its feasible region. Some eigenvalues with null real part are present in the left border ($\theta = 0$), where E_7 becomes unfeasible or possibly bifurcates with other unfeasibile steady states. Both cases fall out of the scope of this study, and hence are not investigated. In addition, several simulations of system (4) have been performed by randomly choosing initial conditions in the interior of $\mathcal{F}$. The average values of the mean square error between the equilibrium E_7 and the asymptotic values of the numerical solution in the feasible region of E_7 is about 10^{-10}. This fact shows numerically that there are no attracting limit cycles in this region, and thus the solutions always converges to E_7. Summarizing, subplot (b) of Fig. 2 reports the feasibility and stability regions for all studied steady state. More specifically, steady states depicted in black are feasible and unstable, while the stable ones are highlighted in blue.
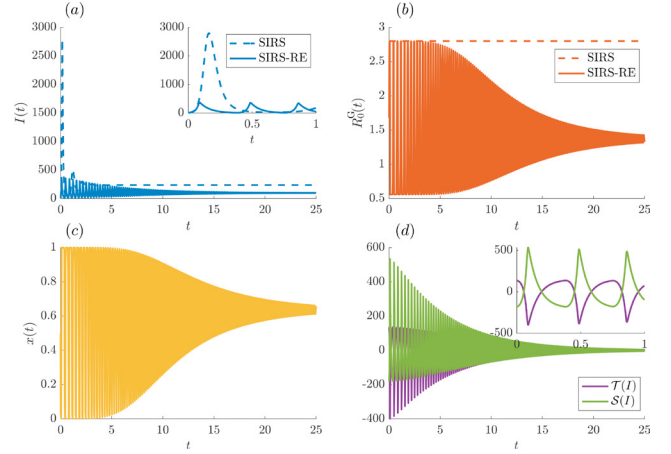

Fig. 3. Comparison of SIRS (1) and SIRS-RE (4) models. (a) Dynamics of the infected individuals $I(t)$. The inset shows a detail of the initial dynamics. (b) basic reproduction number $R_0^G(x)$. (c) propensity to cooperate x. (d) $\mathcal{T}(I)$ and $\mathcal{S}(I)$.

It is interesting to notice that equilibria E_6 and E_7 arise thanks to the presence of the game. Moreover, their I components are lower than the corresponding one of E_4, which is a non null equilibrium also for the SIRS model. Indeed, $E_{6,1} = \underline{\theta} < \overline{\theta} = E_{4,1}$, and $E_{7,1} \leq \overline{\theta}$. Thus, the effect of the cooperation on the pandemic corresponds to a reduced number of infected individuals at steady state. Additionally, the effect of the game can be observed also at the level of the maximum peak reached by I:

$$\hat{I} = N - \hat{R} - \frac{\gamma N}{\beta(x)} \leq N - \hat{R} - \frac{\gamma N}{\beta_0} = N\left(1 - \frac{1}{R_0}\right) - \hat{R},$$

where the last term corresponds to the peak value reached without game, or equivalently when all members of the population defect. It is worthwhile noticing that equilibrium E_4 corresponds to the endemic steady state of the standard SIRS model. Since for $\theta > \overline{\theta}$ E_4 is the unique

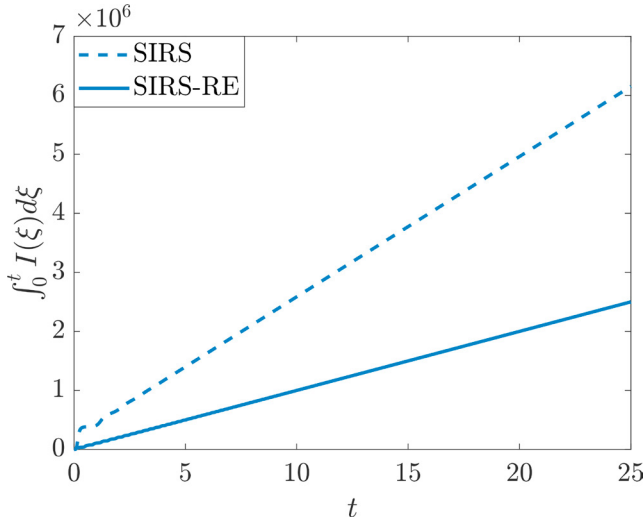Fig. 4. Comparison of SIRS (1) and SIRS-RE (4) models. (a) Dynamics of the cumulative infected individuals $\int_0^t I(\xi)d\xi$.

asymptotically stable equilibrium, and its stability does not depend on the value of m (see Fig. 2), then the virtuous mechanisms produced by cooperative behaviors are not activated. This has a notable epidemiological consequence: in order to design effective containment measures, the policy makers should ensure that the threshold θ is smaller than the baseline endemic value of I.

In subplot (a) of Fig. 3 the time evolution of $I(t)$ for the SIRS (dashed line) and for the SIRS-RE (solid line) are reported. As aforementioned, the first peak (see inset) and the asymptotic value are smaller in the SIRS-RE case, while the frequency of pandemic waves increases. Subplot (b) of Fig. 3 reports the time evolution of the basic reproduction number in both models. It can be appreciated that the oscillating behavior produces time intervals in which the basic reproduction number is smaller than 1, and hence there are time ranges in which the strength of the infection is strongly reduced. Accordingly, subplot (c) of Fig. 3 depicts the time evolution of the cooperation $x(t)$ for the SIRS-RE model. Also in this case, we observe alternating cooperative and defective behaviors in the population. Finally, in subplot(d) of Fig. 3 we report the evolution of the payoff parameters $\mathcal{T}(I)$ and $\mathcal{S}(I)$, showing the succession of phases where the population plays a prisoner's dilemma game, and phases where the game played is the harmony one. The inset reports a zoom on the first year of simulation, allowing to better appreciate the variations of these quantities. Fig. 4 shows that the cumulative amount of infected individuals over time for the SIRS-RE (solid line) is significantly lower than the SIRS case (dashed line).

Bifurcations

The findings of this study can be summarized as follows:

- A transcritical bifurcation occurs between E_4 and E_7 for $\theta = \bar{\theta}$.
- A transcritical bifurcation occurs between E_6 and E_7 for $\theta = \underline{\theta}$.

4. THE SIRS-RE MODEL WITH SEASONALITY

It is reasonable to assume that the contagion follows a seasonal behavior. This can be embedded in the SIRS-RE model by introducing a periodic forcing of period $T = 1$ year. Since there exists the internal steady state E_7, nearby which oscillations are formed, it is interesting to check whether any limit cycle is present under the effect of a seasonally changing parameter R_0^G.

A forcing function, modeling a time varying infection rate according to a seasonal periodicity, is introduced as follows:

$$\beta(x) = \beta_0(1 - mx)\left(1 - \varepsilon \sin\left(\frac{2\pi t}{T} + \phi\right)\right). \quad (7)$$

An extensive simulation analysis of the forced systems has been carried out, by setting the model parameters as in Section 3. Specifically, we set $\phi = 0$ and we vary $\varepsilon \in [0.005, 0.15]$.

As the effect of the seasonality on the infection rate increases, period doubling bifurcations of period T, $3T$, $6T$, $\ldots$, are observed, as reported in subplots (a)-(c) of Fig. 5. For $\varepsilon = 0.119$ a chaotic strange attractor is also present (subplot (d)). These findings suggest that, when dealing with seasonal epidemic, the onset of new infections in future years must be expected. Moreover, when the periodicity is strong enough, predicting the timing of re-infections may be difficult due to the presence of chaotic dynamics in the system.
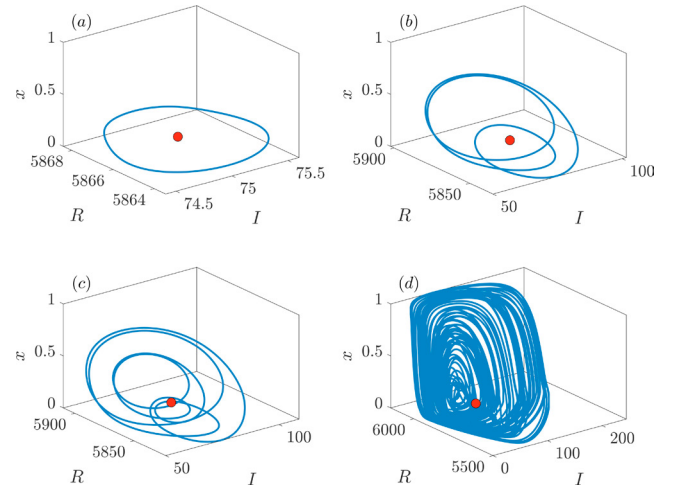

Fig. 5. Route to chaos in the seasonal system (4)-(7) for $N = 10^4$, $\beta_0 = 73$ year^{-1}, $\gamma = 26.1$ year^{-1}, $\alpha = 0.33$ year^{-1}, $\mathcal{T}^0 = 1.5$, $\mathcal{S}^0 = -2$, $\phi = 0$, $m = 0.9$ and $\theta = 75$. The red points represents steady state E_7. (a) $\varepsilon = 0.02$: limit cycle of period T. (b) $\varepsilon = 0.09$: limit cycle of period $3T$. (c) $\varepsilon = 0.11$: limit cycle of period $6T$. (d) $\varepsilon = 0.119$: chaotic attractor.

Stronger values of the parameter ε may induce the extinction of the virus, thus destroying the pandemic. Fig. 6 reports the simulation of the variables $I(t)$ and $x(t)$ for $\varepsilon = 0.6$ and $\theta = 50$. It can be noticed that after some epidemic peaks the disease is fully wiped out. The mechanism explaining the phenomenon is the interplay between the propensity towards cooperation $x(t)$ and the strength of the infection $I(t)$ over time. Indeed, significantly high val-

ues of I foster the cooperation and a successive reduction of the infection itself. The mechanism repeats four times, corresponding to two infection peaks per year, before the convergence of the variables towards vanishing epidemic steady states.
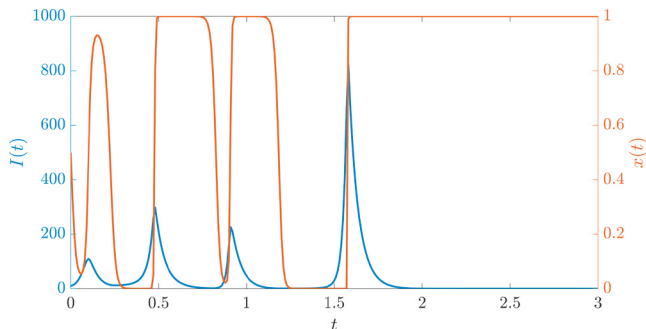

Fig. 6. Defeating the pandemic. Strong values of the seasonality in the SIRS-RE system (4)-(7) induce the extinction of the virus. The parameters setting is the same as in Fig. 5, except for $\theta = 50$ and $\varepsilon = 0.6$.

5. CONCLUSION

This paper presents an extended model, called SIRS-RE, which integrates a standard epidemic SIRS model and the evolutionary game equation RE, which describes the propensity of people to be cooperative, thus adopting the measures taken to control the pandemic. The resulting model assumes that the infection rate decreases when the cooperation rises, while the propensity to cooperate is favoured by strong infection levels, ruled by the threshold parameter θ which embodies the awareness of people on the gravity of the current sanitary crisis. The obtained model shows that the interplay between control measures and infection gravity produces transitory oscillating behavior converging asymptotically towards low infection values. In particular, the succession of epidemic peaks is the result of the alternating phases human/epidemic behaviors. As a results, the dramatic peak of the SIRS model is drastically reduced in the SIRS-RE case; moreover, the cumulative number of infected people is also successfully contained. Moreover, the dependence on seasonality in the infection rate induces chaos, thus showing rich aperiodic behavior in the long run. Finally, for larger values of the parameters defining the seasonal function, the epidemic is also seen to coalesce. As a further development, the authors are investigating the impact of "imperfect information" on the described process. Indeed, it is well known that some of the infectious individuals are pauci- or even a-symptomatic. Additionally, information provided on the status of the pandemics can be also incorrect for the difficulties inherent to the data collection, or for the diffusion of fake news. As a natural consequence, it would be interesting to analyze the system behavior by considering only the fraction of (supposedly) known infectious individuals.

REFERENCES

Augeraud-Véron, E. & Sari, N. (2014). Seasonal dynamics in an SIR epidemic system. J Math Biol, vol. 68, pages 701–725.

Boyd, R., Gintis, H. & Bowles, S. (2010). Coordinated punishment of defectors sustains cooperation and can proliferate when rare. Science, vol. 328, pages 617–620.

Calafiore, G.C., Novara, C. & Possieri, C. (2020). A Modified SIR Model for the COVID-19 Contagion in Italy. 59th IEEE Conference on Decision and Control (CDC), pages 3889–3894.

Della Rossa, F., Salzano, D., Di Meglio, A. et al. (2020). A network model of Italy shows that intermittent regional strategies can alleviate the COVID-19 epidemic. Nat Commun 11, pages 5106.

Funk, S., Salathé, M. & Jansen, V.A.A. (2010). Modelling the influence of human behaviour on the spread of infectious diseases: a review. J R Soc Interface, vol. 7, pages 1247–1256.

Gatto, M., Bertuzzo, E., Mari, L., Miccoli, S., Carraro, L., Casagrandi, R. & Rinaldo, A. (2020). Spread and dynamics of the COVID-19 epidemic in Italy: Effects of emergency containment measures. PNAS, 117 (19), pages 10484–10491.

Hethcote, H.W. (2000). The Mathematics of Infectious Diseases. SIAM Rev., 42(4), pages 599–653.

Hofbauer, J. & Sigmund, K. (2003). Evolutionary game dynamics, Bulletin of the American mathematical society, vol. 40, pages 479–519.

Hofmann, L.M. & Chakraborty, N. & Sycara, K. (2011). The evolution of cooperation in self-interested agent societies: a critical study. In The 10th International Conference on Autonomous Agents and Multiagent Systems, vol. 2, pages 685–692.

Killingback, T. & Doebeli, M. (2002). The continuous prisoner's dilemma and the evolution of cooperation through reciprocal altruism with variable investment. The American Naturalist, vol. 160, pages 421–438.

Madeo, D. & Mocenni, C. & Moraes, J.C. & Zubelli, J.P. (2019). The role of self-loops and link removal in evolutionary games on networks. Math. Biosci. Eng., vol. 16, pages 5287–5306.

Madeo, D. & Mocenni, C. (2020). Self-regulation versus social influence for promoting cooperation on networks. Sci. Rep., vol. 10, pages 4830.

McAdams, D. (2020). Nash SIR: An economic-epidemiological model of strategic behavior during a viral epidemic. Covid Econ, (forthcoming).

Nowak, M.A. & Sigmund, K. (2004). Evolutionary dynamics of biological games. Science, vol. 303, pages 793–799.

Ohtsuki, H., Hauert, C., Lieberman, E. & Nowak, M.A. (2006). A simple rule for the evolution of cooperation on graphs and social networks. Nature, vol. 441, pages 502–505.

Pennisi, E. (2009). On the origin of cooperation. Science vol. 325, pages 1196–1199.

Santos, F.C. & Pacheco, J.M. (2005). Scale-free networks provide a unifying framework for the emergence of cooperation. Phys. Rev. Lett., vol. 95, pages 098104.

Stiff, C. (2020). The game theory of panic-buying – and how to reduce it. The Conversation, UK.

Strogatz, S.H. (2018). Nonlinear dynamics and chaos. CRC press.

Ye, M., Zino, L., Rizzo, A. & Cao, M. Game-theoretic modeling of collective decision making during epidemics. Phys. Rev. E, vol. 104, pages 024314.